



HAL
open science

Supramolecular bioconjugation strategy for antibody-targeted delivery of siRNA

Manon Ripoll, Héloïse Cahuzac, Igor Dovgan, Sylvain Ursuegui, Patrick Neuberg, Stephane Erb, Sarah Cianférani, Antoine Kichler, Jean-Serge Remy,
Alain Wagner

► **To cite this version:**

Manon Ripoll, Héloïse Cahuzac, Igor Dovgan, Sylvain Ursuegui, Patrick Neuberg, et al.. Supramolecular bioconjugation strategy for antibody-targeted delivery of siRNA. *Bioconjugate Chemistry*, 2024, Online ahead of print. 10.1021/acs.bioconjchem.4c00304 . hal-04728199

HAL Id: hal-04728199

<https://hal.science/hal-04728199v1>

Submitted on 9 Oct 2024

HAL is a multi-disciplinary open access archive for the deposit and dissemination of scientific research documents, whether they are published or not. The documents may come from teaching and research institutions in France or abroad, or from public or private research centers.

L'archive ouverte pluridisciplinaire **HAL**, est destinée au dépôt et à la diffusion de documents scientifiques de niveau recherche, publiés ou non, émanant des établissements d'enseignement et de recherche français ou étrangers, des laboratoires publics ou privés.

Supramolecular Bioconjugation Strategy for Antibody-Targeted Delivery of siRNA

Manon Ripoll,[†] Héloïse Cahuzac,[†] Igor Dovgan, Sylvain Ursuegui, Patrick Neuberg, Stephane Erb, Sarah Cianféroni, Antoine Kichler, Jean-Serge Remy, and Alain Wagner*



Cite This: <https://doi.org/10.1021/acs.bioconjchem.4c00304>



Read Online

ACCESS |



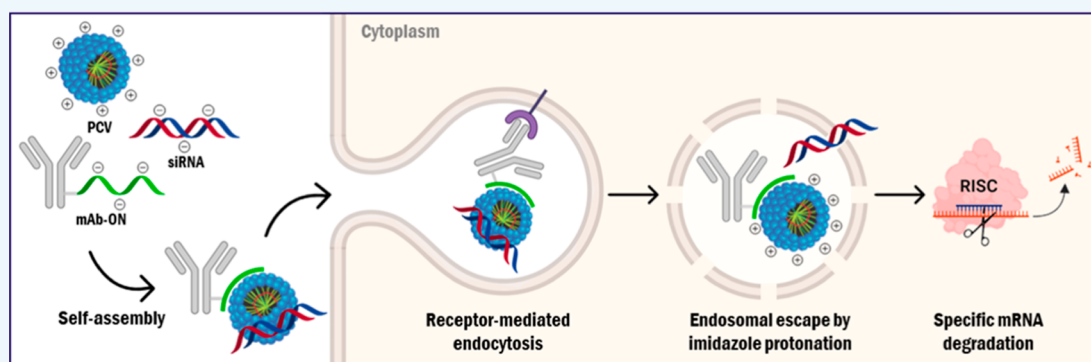
Metrics & More



Article Recommendations



Supporting Information



ABSTRACT: RNA interference is a widely used biological process by which double-stranded RNA induces sequence-specific gene silencing by targeting mRNA for degradation. However, the physicochemical properties of siRNAs make their delivery extremely challenging, thus limiting their bioavailability at the target site. In this context, we developed a versatile and selective siRNA delivery system of a trastuzumab-conjugated nanocarrier. These immunoconjugates consist of the assembly by electrostatic interactions of an oligonucleotide-modified antibody with a cationic micelle for the targeted delivery of siRNA in HER2-overexpressing cancer cells. Results show that, when associated with the corresponding siRNA at the appropriate N/P ratio, our supramolecular assembly was able to efficiently induce luciferase and PLK-1 gene silencing in a cell-selective manner *in vitro*.

INTRODUCTION

Over the last decades, antibody–drug conjugates (ADCs) have demonstrated the outstanding potential of targeted medicines in the field of oncology and have stimulated novel strategies for antibiotics and immunomodulation.¹ Hence, trastuzumab, first approved for clinical use in 1998, paved the way toward what seemed to be a general strategy for bioactive compound delivery, as shown by the exploding number of ADCs reaching clinics in recent years (from 25 in 2012 to more than 170 in 2022).² Disappointingly, however, many ADCs fail during clinical development due to excessive toxicities and unfavorable risk–benefit profiles. Indeed, mechanisms such as premature release of the cytotoxic payload within the systemic circulation or nonspecific uptake of ADCs in healthy tissues contribute to narrow their therapeutic window.³ Thorough research projects were thus engaged and are still ongoing in order to improve ADC tolerability, which will prepare the next generation of antibody-targeted therapeutics. Virtually, all pits for improvement were systematically reviewed, and accordingly engineered antibodies and alternative antibody formats, controlled conjugation methods, and more stable and soluble linkers were developed.⁴

In this context, clinicians were looking for the ideal toxic payload that would be deprived of systemic toxicity while inducing death only upon antibody-triggered internalization into cancer cells. Obviously, small interfering RNAs (siRNAs) that have an impact on the cell cycle through a specific RNA interference mechanism fall into the class of cytostatic molecules that could fulfill these criteria.⁵ Thanks to its biological activity, antiproliferative siRNA can address a wide panel of mode of actions and improve efficacy through synergistic effects when combined with small anticancer drug molecules.⁶ Nevertheless, there are various challenges that limit siRNA bioavailability at the target site. Indeed, due to their high molecular weight and their multiple negative charges, naked siRNAs are unable to cross biological membranes. Moreover, nonchemically modified siRNAs

Received: July 2, 2024

Revised: September 17, 2024

Accepted: September 19, 2024

Scheme 1. Supramolecular Assembly Strategy to Provide Tunable Multifunctional Targeted Vector

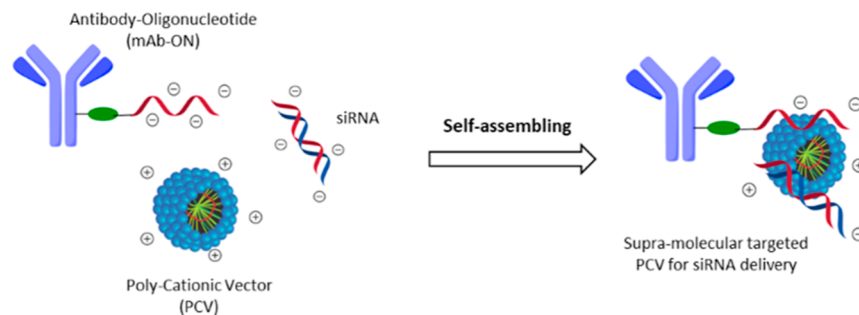


exhibit a poor plasmatic stability, with an average half-life of between 5 and 10 min.⁷ Hence, an efficient siRNA delivery system should be able to protect it from plasma degradation while targeting it to its site of action.

Compared to small-molecule drugs, siRNA requires a multifunctional system in order to achieve protection from plasmatic nucleases, targeting toward specific cell types, as well as internalization and release in the cytosol after escaping lysosomal processing that could also degrade it. Traditional strategies for targeted siRNA delivery rely on covalent conjugation of targeting agent that could be either small molecules (folic acid,⁸ cRGD peptides,⁹ and anisamide analogues¹⁰) or biologics (aptamers,¹¹ antibody and antibody fragments,¹² or DARPin¹³) or on encapsulation of the therapeutic siRNA into a nanocarrier such as a stimuli-responsive polymer,¹⁴ a dendrimer,¹⁵ or a lipid assembly¹⁶ that could be coated with the above-mentioned targeting agents. The chemical conjugation of those targeting moieties, which differ in their molecular weight, amino acid composition, and functional nanoconstructs, requires, however, a lengthy optimization due to (i) the stochastic nature of chemical reaction on multifunctional biomolecules, (ii) hydrolytic reagents and plasmatic instability, and (iii) difficult purification of the final nanovector, providing an inaccurate quality control of the final formulation and a high batch-to-batch variability.

Recent strategies that bypass the difficulties of this chemical coupling step have therefore emerged. Among those, Fab or scFv-protamine fusions provided molecularly defined biomolecules ready to be used for siRNA loading without any chemical bioconjugation step.^{17,18} These biomolecule-based approaches lack somehow adaptability and modularity that are necessary to fine-tune delivery, efficacy, and specificity. In a future directed personalized medicinal approach, an optimized delivery construct would include modularity in its targeting moieties in order to allow for a personalized medicine. Thus, despite their complexity, chemobiological systems are still considered as the most promising approaches. Novel generation of modular platforms that enables a targeted delivery of siRNA using self-assembling nanocarriers were thus recently disclosed. These systems are based on a membrane-anchored lipoprotein that is incorporated into siRNA-loaded lipid nanoparticles that interact with the Fc domain of antibodies¹⁹ or on a mixture of antibody-protamine, free SMCC-protamine, and siRNA that spontaneously forms vesicular nanoparticles.²⁰ Intact siRNA, after cellular uptake, is then delivered into the cytosol thanks to early endosomal release.

Furthermore, one family of nontargeted siRNA vectors that are used in research are based on polycationic molecules that compact RNA, internalize into cells via endocytosis, and

release intact RNA in the cytosol via the so-called “proton sponge” effect.^{21,22} Although very efficient, in terms of RNA transfer, plain polymeric cationic vectors lack cell selectivity. They are often limited in use because of their poor compatibility with serum media. Due to their polydispersity and heterogeneity, polymers are even less amenable to reproducible chemical derivatization than chemically well-defined targeted lipid constructs. We thus thought to develop a new versatile approach of the noncovalent conjugation system that would enable reliable and versatile coassembly of a targeting antibody and a bioactive siRNA onto a nanostructured polycationic vector. This would allow easy access to a tunable construct showing high cell specificity and good plasmatic compatibility.

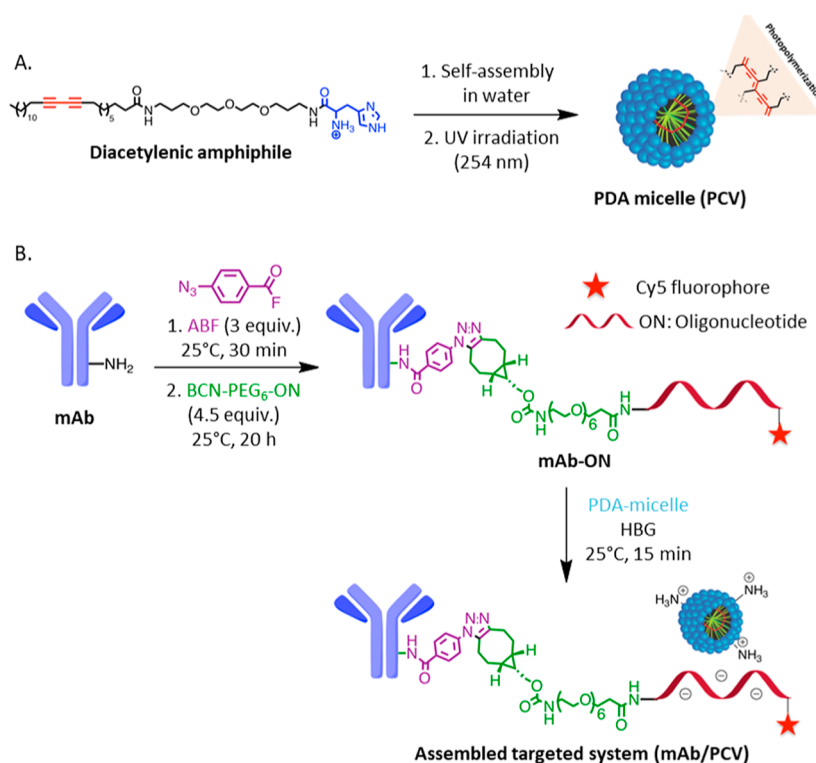
We have based the design of such a system on our recent demonstration that an antibody–oligonucleotide conjugate (mAb-ON) electrostatically sticks onto polycationic nanoparticles with sufficient strength in order to form a serum stable antibody toxic nanoparticle conjugate.²³ Then, we hypothesized that a tricomponent formulation of a mAb-ON, a siRNA, and a polycationic nanovector (PCV) would provide a theoretically unlimited repertoire of siRNA-targeted carriers (Scheme 1). Such an approach would enable one to easily adjust the characteristics of the vector by changing the ratios of the different components in the formulation. In addition, the idea of starting with individually characterized noncovalently linked components would favor the nanovector to disassemble in the endosome and release intact siRNA bearing no chemical modification. This supramolecular assembly would also enable a higher quality control due to better characterization of the individual components.

Herein, we show that such a conjugation strategy—by decorating our nanovectors with mAb-ON—is indeed shielding the positive and negative charges of the PCV and the siRNA, respectively, that otherwise could lead to unspecific internalization in cancer cells.²⁴ Moreover, the compatibility with serum has been demonstrated.

RESULTS AND DISCUSSION

Synthesis of the PCV. As PCV, we decided to investigate nanometric photopolymerized polydiacetylenic (PDA) micelles.^{25–27} We previously demonstrated that these nanocarriers have a high capacity to deliver siRNAs into cells.^{26,27} This delivery system indeed appears as a good candidate since it shows low toxicity and nanometric size and is able to complex siRNA at low N/P ratio, calculated stoichiometrically as the mole ratio of the cationic amphiphilic compound (1 positive charge per molecule) to siRNA nucleotide residue (42 negative charges per siRNA)—with high reproducibility.

Scheme 2. (A) PDA–Micelle Formulation. (B) Supramolecular Assembly Strategy of the Targeted System for siRNA or Drug Delivery



These PDA–micelles were obtained after UV irradiation of self-assembled diacetylenic amphiphiles that contain a histidine moiety as a protonable hydrophilic head (Scheme 2A). After extensive dialysis of the PDA–micelle to remove traces of nonpolymerized monomers, responsible for possible vector toxicity,²⁶ micelles were diluted at 1 mg/mL (1.4 mM) and stored at 4 °C. Previous results have shown that photopolymerization is the key step in PDA–micelle formulation, enabling highly stable micellar structures to be obtained, which translates into a lower CMC (critical micelle concentration) value compared to the nonpolymerized form.²⁸ Also, in water, the photopolymerized micelles exhibit a zeta potential of +60 mV (Figure S1), indicating that particles are highly charged, which prevent aggregation and ensure redispersion due to repulsive electric force, making it a stable nanoformulation.²⁹ Indeed, we found that this stock solution in water could be kept for more than six months at 4 °C with no change in size and surface charges (data not shown). Their great stability and positively charged surface, providing the ability to electrostatically stick to negatively charged oligonucleotides, as well as their size (around 10 nm²⁶) that is similar to the one of the antibody, make photopolymerized PDA–micelles a model of choice of PCV to demonstrate the proof of concept.

Synthesis of the Antibody–Oligonucleotide Conjugate. As a polyanionic tail for grafting on the mAb, we decided to use a 37-mer single-stranded oligonucleotide. Oligonucleotides are indeed suitable candidates for the design of such a “sticking moiety”. They are natural biopolymers whose degradation should involve minimal release of xenobiotic metabolite, thus reducing the possible undesired toxicity and side effect. The sequence of this oligonucleotide was designed to avoid any intrinsic biological activity to ensure that the observed activities result only from the delivered siRNA.

As a biological model system, we selected as an active targeting antibody trastuzumab (T), an anti-HER2 monoclonal antibody used in human medicine for the treatment of breast cancer.³⁰ This mAb was chosen to selectively target the HER2-expressing human breast cancer cells SK-BR-3. As control, a nontargeting mAb, rituximab (R), that targets CD20 (not expressed in SK-BR-3) was selected. Thus, we expect to specifically deliver the siRNA in SK-BR-3 with a T-coated vector, while no delivery should be observed neither in non-HER2 expressing cells (human breast cancer cells MDA-MB-231) nor when using a vector coated with a nontargeting R antibody.

The synthesis of mAb-ON was realized in two steps based on the “plug and play” strategy developed in our group.³¹ Briefly, both T and R antibodies were reacted with 3 equiv of 4-azidobenzoyl fluoride (ABF) in phosphate-buffered saline (PBS) 1× buffer at 25 °C for 30 min yielding azide-modified antibodies, named, respectively, T-N₃ and R-N₃. These adducts were characterized by native MS analyses and have showed an average degree of conjugation (DoC) of 2.1 (Figure S2) as previously described.³¹ In parallel, starting from a 37-bases 5′-amino-modified oligonucleotide (ON) bearing a Cy5 fluorophore at the 3′ end, we prepared a functionalized oligonucleotide BCN-PEG₆-ON bearing a bicyclononyne (BCN) group as a strained alkyne (Figure S3). It was then involved in a strain-promoted azide–alkyne cycloaddition (SPAAC) with the azide-modified antibodies T-N₃ and R-N₃ overnight at 25 °C to afford, after purification by size exclusion chromatography (SEC), mAb-ON, abbreviated as T-ON and R-ON for trastuzumab and rituximab, respectively. The average DoC was consistent with that of the original mAb-N₃ and estimated at 2.1 as calculated by in-gel fluorescence and SEC-MS analysis of the conjugates (Figure S4). This strategy

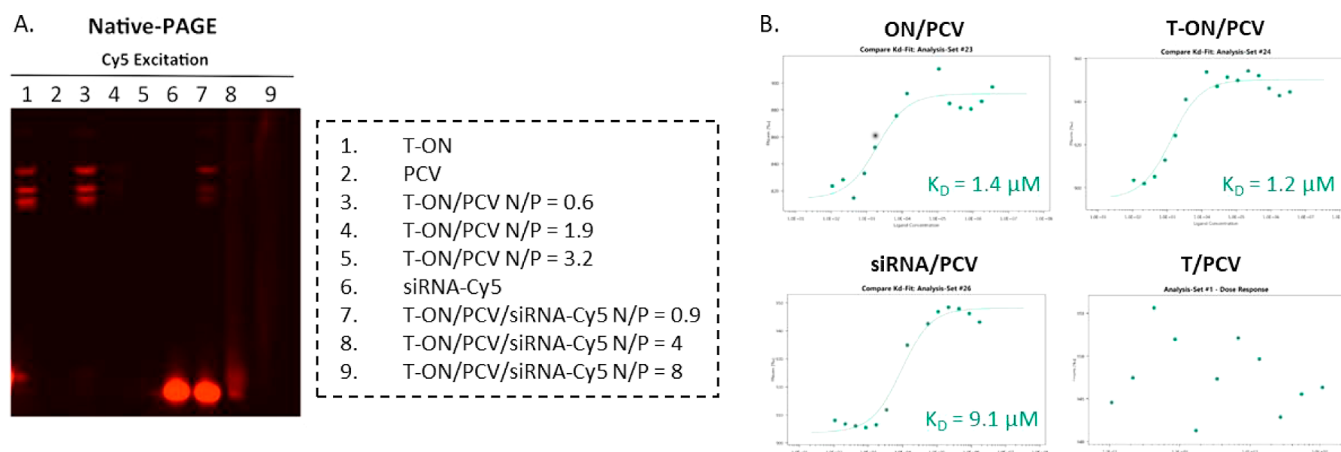


Figure 1. (A) siRNA and mAb-ON/PCV complexation at different molar ratios. Analysis by gel electrophoresis using native-PAGE with tris-acetate buffer (pH = 7.5). T-ON appears as three bands corresponding to the separated DoC1, DoC2, and DoC3 species leading to a final DoC2.1 mixture. (B) Dissociation constants measured by thermophoresis between ON-Cy5 and PCV, T-ON-Cy5 and PCV, siRNA-Cy5 and PCV, and as a negative control between trastuzumab labeled with TAMRA and the PCV.

thus permits to obtain rapidly and reliably tunable anionic moieties having HER2 receptors targeting properties.

For further N/P ratio calculations, we will thus consider that our mAb-ON has an average DoC of 2.1, and as it was grafted with a single-strain ON of 37 bases long, it will thus account for about 78 negative charges.

Assembly of the Tricomponent HER2-Targeted siRNA Delivery System. The molecular assembly step between the polyanionic mAb-ON (T-ON or R-ON), the siRNA, and the polycationic nanocarrier was performed in a two-step sequence by first adding the PCV (1 mg/mL) to a solution of mAb-ON (0.2 mg/mL stock solution) prediluted in 5% HEPES-buffered glucose. Then, after 15 min of gentle mixing at room temperature, the siRNA (5 μM stock solution in RNase free water) was added and mixed for an additional 1 h. The solution was then vortexed and incubated for 45 min at room temperature before use. For this formulation, a new N/P ratio was calculated according to the following equation

$$\frac{N}{P} = \frac{n(\text{monomer})}{n(\text{siRNA}) \times 42 + n(\text{mAb} - \text{ON}) \times 37 \times \text{DoC}}$$

The added quantity of each component was calculated in order to respect a N/P ratio of 10 between the PCV and the siRNA and a global N/P ratio of 6 in the presence of mAb-ON. These ratios were determined according to the *in vitro* optimization (Figures S5 and S6) and the gel mobility shift assay (see below).

Characterization of the mAb-ON/PCV Conjugate. In order to have an optimized design of our nanoconstructs, we first investigated the stability of the assembly that is kept together only through noncovalent electrostatic interactions. First, T-ON (1.5 μg) was mixed with different ratios of PCV (0.6 μg , 1.8 μg , and 3 μg , which correspond, respectively, to N/P ratios of 0.6, 1.9, and 3.2) to identify the lowest N/P ratio that allows full complexation of mAb-ON. To this end, native-PAGE gel was formed using tris-acetate buffer (pH 7.5) as the running buffer, enabling to maintain the protonation of the cationic vector. As shown in Figure 1A, the PCV is able to totally complex T-ON by electrostatic interactions at a N/P ratio of at least 1.9 (columns 4 and 5), while at N/P = 0.6 (column 3), migration of free T-ON was still visible. Next, we evaluated the stability of the assembly when part of the

negative charges (P) brought by mAb-ON was substituted by charges coming from a siRNA. Therefore, we maintained a constant amount of negative charges by setting the ratio between T-ON and siRNA to 1.5, while increasing amounts of PCV were added to obtain increasing N/P values. In this context, a Cy5-labeled siRNA was mixed with the preformed mAb-ON/PCV complex. In the case of this ternary mixture, we observed that a N/P ratio higher than 4 was necessary to have total complexation, demonstrated by the lack of the Cy5 signal (Figure 1A, columns 8 and 9) resulting from charge neutralization. These gel mobility shift results are in line with the measurement of a 0 mV zeta potential for the ternary complex T-ON/PCV/siRNA formulated at an overall N/P ratio of 4 (Figure S7A). Furthermore, the DLS analysis of the same conjugate showed a size distribution by the number centered at around 419 nm (Figure S7B), confirming that the ternary complex retains a nanometric size.

To further characterize the affinity of mAb-ON with PCV, we performed thermophoresis experiments (Figure 1B). To this end, the concentrations of the different biomolecules (siRNA, ON, or T-ON) were kept constant, while the concentration of the nonlabeled PCV was varied from 3.5 mM to 0.1 μM . The affinity of the PCV with either the free Cy5-labeled 37-mer oligonucleotide (ON/PCV), the T-ON-Cy5 conjugate (T-ON/PCV), the siRNA-Cy5 (siRNA/PCV), and the nonconjugated trastuzumab labeled with TAMRA (T/PCV) were measured in HBG using the monolith NT.115 instrument. First, we observed no interaction between the naked mAb control T-TAMRA and the PCV, which confirms the requirement of the anionic oligonucleotide to form the complex. Regarding the other components, the dissociation constants fall all in the micromolar range, which is characteristic of such electrostatic interactions.²⁶ Interestingly, we noticed that the 37-mer single-strand oligonucleotide has a slightly better affinity for the PCV as compared to the double-stranded siRNA (respectively, 1.4 and 9.1 μM). Finally, we demonstrated that the conjugation of the ON to trastuzumab did not alter the affinity between the ON and the PCV, as the K_D values were similar. We then decided to evaluate the efficacy of these supramolecular complexes to target cells *in vitro*.

In Vitro Imaging. To assess the cell selectivity profile and to conclude on whether our supramolecular assembly would favor specific delivery into antigen presenting cells and limit siRNA delivery in nontarget cell lines, various fluorescent-labeled conjugates were analyzed by confocal microscopy on overexpressing HER2 (HER2+) SK-BR-3 cells and non-expressing HER2 (HER2-) MDA-MB-231 cells. To this end, we prepared T-ON and R-ON labeled on the DNA strand with a Cy5 fluorophore, and a siRNA payload bearing a Cy3 fluorescent label was added. Both mAb-ON-Cy5 and siRNA-Cy3 and PCV were mixed with the tertiary complex at a N/P ratio of 6. After 3 h of incubation at 37 °C, cells were washed with PBS, stained with DAPI, and imaged by confocal microscopy.

As expected, we observed that T-ON/PCV was able to efficiently deliver the fluorescently labeled siRNA into HER2+ cells (Figure 2, second column). The colocalization observed

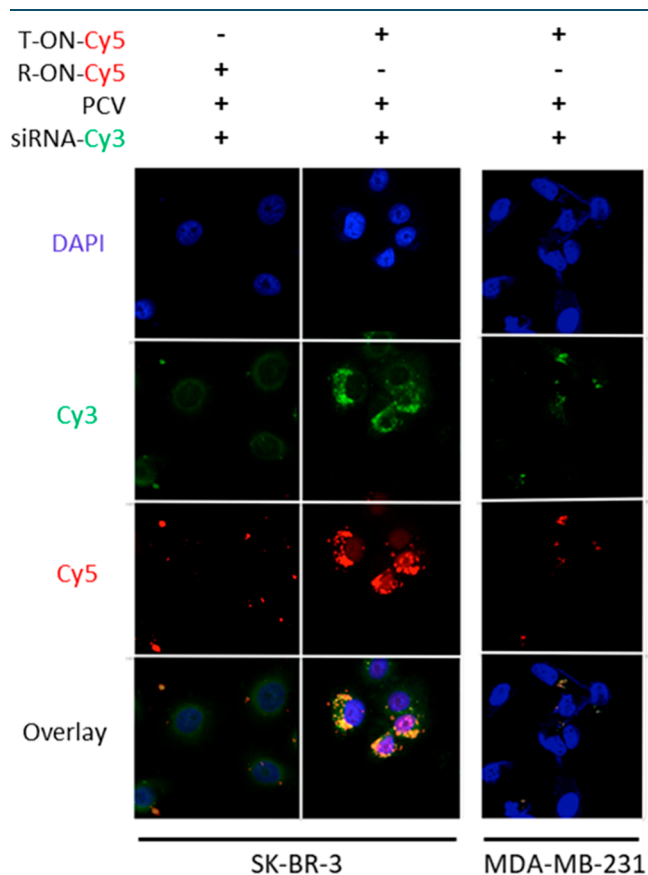


Figure 2. T-ON/PCV conjugate selectively internalizes into SK-BR-3 breast cancer cells. Confocal microscopy images of SK-BR-3 (HER2+) and MDA-MB-231 (HER2-) cells after incubation with labeled compounds for 3 h at 37 °C. (Lasers used: DAPI 405 nm, Cy3 561 nm, and Cy5 635 nm, objective 63 \times .) Image size: 367.83 μm \times 367.83 μm .

between the Cy5-labeled mAb-ON and the siRNA-Cy3 indicates that the whole ternary complex was internalized into cells. Satisfactorily, we also observed considerably less intense Cy3 and Cy5 fluorescence signals in the case where R-ON/PCV/siRNA was incubated on SK-BR-3 cells (Figure 2, 1st column) and when the trastuzumab-based T-ON/PCV/siRNA conjugate was incubated on the HER2- cell line (Figure 2, 3rd column). Taken together, these results confirm that the internalization of the complex is predominantly

triggered by receptor-mediated endocytosis, although non-specific mechanisms of uptake are also involved in a lesser extent, most likely due to nonspecific interactions with cell membranes.²⁴

As all these results clearly evidenced that our tricomponent assembly allows cell targeting, we next wanted to investigate whether our construct would enable the efficient delivery of a functional siRNA into cells.

In Vitro Evaluation. We performed the in vitro evaluation of the ability of T-ON/PCV to deliver functional siRNAs on the two cell lines SK-BR-3-Luc and MDA-MB-231-Luc that stably express the luciferase gene and that are HER2+ and HER2-, respectively. As a siRNA payload, we used a siRNA targeting the luciferase gene (siLuc). Thus, when siLuc is delivered into the cytoplasm, a knockdown of the luciferase expression that would be quantified by a decrease of the luciferase bioluminescence signal is expected. 50 nM siRNA (siLuc or siCtrl) was mixed with T-ON/PCV or R-ON/PCV to obtain a final N/P ratio of 6. The resulting nanoconstructs were then incubated in SK-BR-3 and MDA-MB-231 cells. The luciferase bioluminescence signal was quantified after 48 h of incubation and is reported in Figure 3A.

Compared to untreated cells (gray bar, Figure 3A), an efficient silencing of luciferase was observed in SK-BR-3-Luc when treated with 50 nM of siLuc conjugated to T-ON/PCV (pink bar, Figure 3A), while no knockdown of the gene was observed with the controls, namely, control siRNA (siCtrl, blue bar) and control antibody-conjugate (R-ON/PCV, green bar) (Figure 3A). Moreover, on HER2- luciferase cells, no significant difference of the expression of luciferase between cells treated with siLuc or siCtrl was observed, meaning that no silencing of the luciferase gene occurred. These results are in line with our previous observation that our targeted assembly is able to specifically internalize in cells in an antibody-dependent manner. Moreover, it also demonstrates that after internalization, this delivery system releases a functional siRNA capable of inducing gene silencing.

Once the proof of concept was established with a reporter gene, we investigated the delivery of a siRNA of therapeutic interest. We turned our attention to a siRNA that targets Polo-Like Kinase 1 (PLK-1). As this protein, which is overexpressed in many cancers, plays a crucial role in the mitosis process, its silencing leads to cell cycle arrest and then to apoptosis.^{32,33} Therefore, quantification of the silencing of the target gene by siPLK-1 was evaluated by the cell viability assay. Experiments were performed on SK-BR-3 (HER2+) and MDA-MB-231 (HER2-) using various siRNA concentrations (1, 10, 20, and 50 nM) but always keeping a mAb/PCV ratio of 2 and a N/P ratio of 6 for the whole tertiary complex. As expected, when HER2+ cells were incubated in the presence of siPLK-1 loaded on T-ON/PCV, the cell viability decreased in a concentration-dependent manner (Figure 3B, pink bars). However, and to a lesser extent, a reduction in cell viability was also noticed in the presence of control antibody conjugates (Figure 3B, green bars) or with HER2- cells (Figure 3B, MDA-MB-231), as a consequence of the minor amount of conjugate that is taken up by the cells in a nonspecific manner, as illustrated in Figure 2. In addition, it should be mentioned that the toxicity of targeted PDA-micelles has been reported,²³ and thus, reduced cell viability can also be attributed to the micelle's intrinsic toxicity (Figure S8).

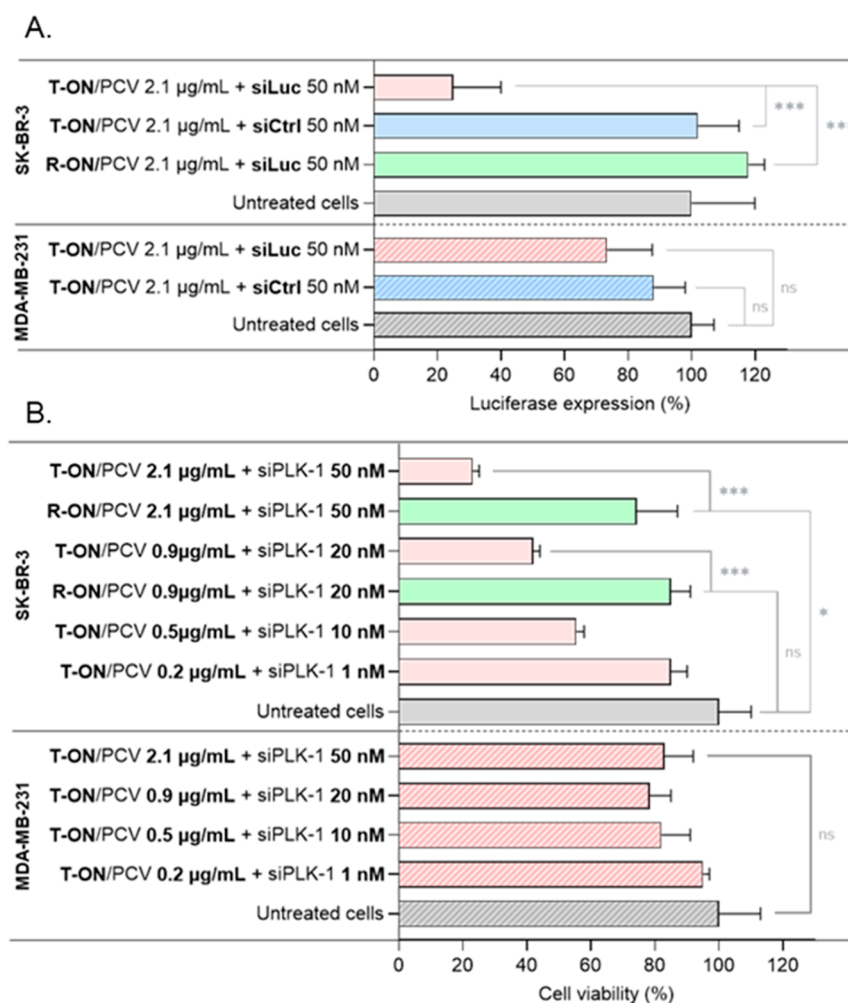


Figure 3. Cell-selective efficient delivery of siRNA in vitro. (A) The delivery of siLuc decreases the luciferase bioluminescence signal in the SK-BR-3 cell line that stably expresses the luciferase gene. (B) The delivery of siPLK-1 induces cell death in a concentration-dependent manner. Values of three independent experiments are reported in the graph bar and are expressed as mean \pm SD. Statistical significance was assessed by one-way ANOVA and Tukey's post hoc analysis (ns $p > 0.05$, * $p < 0.05$, ** $p < 0.01$, and *** $p < 0.001$).

CONCLUSIONS

In this paper, we describe an original supramolecular assembly strategy that enabled us to stick together a targeting agent, a bioactive siRNA, and an endosome-disrupting PCV. Hence, we demonstrated that a cationic vector can be associated with an oligonucleotide-modified antibody via electrostatic interactions while keeping the ability to complex siRNAs. We further showed that, when associated with the corresponding siRNA at an appropriate N/P ratio of 6, a trastuzumab-ON-PCV conjugate was able to efficiently induce luciferase and PLK-1 gene silencing. Beyond the trastuzumab/SK-BR-3 cancer model we have used in this study, the reported system opens interesting perspectives because of its high versatility, allowing, in theory, to combine almost any RNA to any DNA-conjugated antibody. In addition, since antibody-RNA conjugates (ARC) demonstrate biological activity on their own,³⁴ such supramolecular conjugation strategy opens new ways to combine easily active ARC and active siRNA at different ratios.

MATERIALS AND METHODS

Oligonucleotides. Oligonucleotides were purchased from IDT. 5'-Amino-modified oligonucleotide bearing a Cy5

fluorophore at the 3'-end for antibody conjugation, sequence: 5'-AAGATACGAATTCGGGTGTTCTGCTGGTAGTGGTTCGG-3'. siLuc, sense: CUUACGCUGA GUA-CUUCGAdTdT, antisense: UCGAAGUACUCAGC-GUAAGdTdT. siPLK-1, sense: 5'-AGA UCA CCC UCC UUA AAU AUU-3', antisense: 5'-UUA UUA AGG GUG AUC UUU-3', in bold, the 2'-O-methylated-modified nucleotides. siCTL sense: 5'-CGU ACGCGG AAU ACU UCG ATT-3', antisense: 5'-U CGA AGU AUU CCG CGU ACG TT-3'.

Synthesis of the BCN-Oligonucleotide. To a solution of amino-modified oligonucleotide (1 nmol/ μ L in DNase/RNase-free water, 1 equiv) were added BCN-PEG₆-PFP (synthesized as previously described)³¹ from a DMSO stock solution (10 mM, 20 equiv) and NaHCO₃ (1 M solution in water, 250 equiv). The mixture was gently stirred at 25 °C for 16 h. LiClO₄ (3 M, one-third of the reaction volume) and cold acetone (3 times the reaction volume) were added to precipitate functionalized siRNA. This step was repeated two times.

Synthesis of Antibody-Oligonucleotide Conjugates (T-ON and R-ON). The antibody modification with azide handles was performed following a previously reported

protocol.³¹ To a solution of mAb (5 mg/mL, 1 equiv) in PBS (1×, pH 7.4) was added 4-azidobenzoyl fluoride (synthesized as previously described³¹) from a 1 mM DMSO solution (3 equiv). The reaction was incubated for 30 min at 25 °C. Excess of reagents was removed by gel filtration using Biospin P-30 columns (Bio-Rad, Hercules, USA) pre-equilibrated with PBS (1×, pH 7.4) to give a solution of mAb-N₃ with an average degree of conjugation of 2.2. BCN-PEG₆-ON resuspended in water (3 equiv) was then added to the solution of mAb-N₃ (2 mg/mL, 1 equiv). The reaction mixture was incubated for 24 h at 25 °C. mAb-ONs were purified by SEC (Superdex 200 increase 10/300, Cytiva), and fractions of interest were concentrated using microconcentrators (Vivaspin, 50 kDa MWCO, Sartorius) to afford final mAb-ON in 50–55% yield. Protein concentration was determined using a BCA Protein Assay Kit (Thermo Fisher Scientific) according to the manufacturer's protocol.

Micelle Formulation. The amphiphile C₂₅-diyne-trioxa-histidine was synthesized using previously reported conditions.²⁶ The formation of micelles was performed by solubilizing 5 mg of amphiphile into a solution of 0.1 N HCl and ethanol (1/5). The solvent was evaporated under reduced pressure until film formation. The film was then solubilized in 1 mL of deionized water and sonicated for 30 min (80 W, 25 °C) to obtain micelles. The solutions were polymerized at various UV irradiation times at 254 nm and 48 W in 1 mL quartz cuvettes into a Cross-Linker Bio-Link 254 (Fisher Bioblock) to obtain the polymerized micelles. The dialyses were performed in 2000 MWCO dialysis cassettes (Thermo Fisher) using a stepwise solvent gradient from 7:3 EtOH/H₂O to pure water in 4 days.

Complexation between siRNA and Micelles. siRNA/micelle complexes were formulated by adding micelles in a solution of siRNA prediluted in HEPES buffer glucose (HBG: pH 7.5, 10 mM HEPES, 10 mM HEPES-Na, and 5% glucose w/v). The mixture was incubated for 1 h at 25 °C before being used.

Formulation of Immune Micelles. Immunomicelles were formulated in HBG by adding various amounts of micelles to mAb-ON. After 15 min of incubation at 25 °C, various amounts of siRNA were added to the previous formulation of immunomicelles to obtain the final ternary assembly after one hour of incubation.

Thermophoresis. The concentration of the labeled siRNA or antibody was kept constant, while the concentration of the nonlabeled micelles was varied between 0.1 μM and 3.5 mM. The assay was performed in HEPES-buffered glucose (5%). After a short incubation, the samples were loaded into MST NT.115 premium glass capillaries, and the MST analysis was performed using the monolith NT.115 NanoTemper.

Size and Zeta Potential Measurements. The hydrodynamic diameters of the micelles or complexes were determined using the Zetasizer Nano ZS system (Malvern Instruments) with the following specifications: material index of refraction = 1.43 (liposome); sampling time = 55 s; refractive index of HBG = 1.337 or water = 1.33; viscosity of HBG = 1.1557 or water = 0.8872; temperature = 25 °C, and using microcuvettes of 90 μL volume. For zeta potential measurement, the same instrument was used with the appropriate cuvettes (1 mL) and an effective voltage of 70 V.

Cell Culture. Human breast cancer cells MDA-MB-231 and SK-BR-3 were cultured in Dulbecco's modified Eagle's medium (DMEM, high glucose, Gibco-Invitrogen) supple-

mented with 10% fetal bovine serum (Eurobio) and 1% antibiotic solution (penicillin–streptomycin, Gibco-Invitrogen) in a 5% CO₂-humidified atmosphere at 37 °C.

Cell Viability Assay. Twenty-four hours prior to the experiment, SK-BR-3 and MDA-MB-231 cells were seeded at a density of 1 × 10⁴ cells per well in 96-well tissue culture plates. On the day of the experiment, compounds in fresh culture medium were added to the cells. Cell viability was measured after 48 h by quantifying the mitochondrial succinate dehydrogenase, using an MTT assay (Invitrogen).

Confocal Microscopy. Twenty-four hours prior to the experiment, SK-BR-3 and MDA-MB-231 cells were seeded at a density of 1 × 10⁴ cells per well in the Lab-tek II chamber slide from Thermo Fisher. Samples were added onto the cells in 200 μL of DMEM supplemented with 10% of serum. After 3 h of incubation, the medium was removed, and the cells were washed twice with PBS. Cells were fixed with a 4% formaldehyde solution in PBS. After 30 min of incubation at room temperature, cells were rinsed with cold PBS and then deionized water. The chamber was removed, and cells were cover-slipped using an aqueous mounting medium containing DAPI (Fluoroshield from Sigma). Confocal microscopy was performed on a Leica SPE confocal microscope 11506513 (lasers used: DAPI 405 nm, Cy3 561 nm, and Cy5 635 nm, objective 63×).

■ ASSOCIATED CONTENT

SI Supporting Information

The Supporting Information is available free of charge at <https://pubs.acs.org/doi/10.1021/acs.bioconjchem.4c00304>.

Analytical data—including HPLC profiles, SEC-nMS profile, and DLS and zeta potential measurements—and in vitro assays (PDF)

■ AUTHOR INFORMATION

Corresponding Author

Alain Wagner – *Bio-Functional Chemistry (UMR 7199), LabEx Medalis, University of Strasbourg, Illkirch-Graffenstaden 67400, France*; orcid.org/0000-0003-3125-601X; Email: alwag@unistra.fr

Authors

Manon Ripoll – *Bio-Functional Chemistry (UMR 7199), LabEx Medalis, University of Strasbourg, Illkirch-Graffenstaden 67400, France*

Héloïse Cahuzac – *Bio-Functional Chemistry (UMR 7199), LabEx Medalis, University of Strasbourg, Illkirch-Graffenstaden 67400, France*

Igor Dovgan – *Bio-Functional Chemistry (UMR 7199), LabEx Medalis, University of Strasbourg, Illkirch-Graffenstaden 67400, France*; orcid.org/0000-0002-1178-8118

Sylvain Ursuegui – *Bio-Functional Chemistry (UMR 7199), LabEx Medalis, University of Strasbourg, Illkirch-Graffenstaden 67400, France*

Patrick Neuberger – *Bio-Functional Chemistry (UMR 7199), LabEx Medalis, University of Strasbourg, Illkirch-Graffenstaden 67400, France*; orcid.org/0000-0003-4444-3623

Stephane Erb – *BioOrganic Mass Spectrometry Laboratory (LSMBO), IPHC, University of Strasbourg, Strasbourg*

67087, France; IPHC, CNRS, UMR7178, University of Strasbourg, Strasbourg 67087, France

Sarah Cianféran – BioOrganic Mass Spectrometry Laboratory (LSMBO), IPHC, University of Strasbourg, Strasbourg 67087, France; IPHC, CNRS, UMR7178, University of Strasbourg, Strasbourg 67087, France;
orcid.org/0000-0003-4013-4129

Antoine Kichler – Université de Strasbourg, Institut National de la Recherche Médicale (INSERM), Centre National de la Recherche Scientifique (CNRS), Biomaterials and Bioengineering, Illkirch 67401, France

Jean-Serge Remy – Bio-Functional Chemistry (UMR 7199), LabEx Medalis, University of Strasbourg, Illkirch-Graffenstaden 67400, France

Complete contact information is available at:

<https://pubs.acs.org/10.1021/acs.bioconjchem.4c00304>

Author Contributions

[†]M.P. and H.C. contributed equally to this work.

Funding

This work was supported by the Labex Medalis and the Interdisciplinary Thematic Institute IMS (Institut du Médicament Strasbourg), as part of the ITI 2021–2028 supported by IdEx Unistra (ANR-10-IDEX-0002) and the SFRI-STRAT'US project (ANR-20-SFRI-0012) under the framework of French Investments for Future Programs. M.R. has received financial support from MESR (Ministère de l'Enseignement supérieur et de la Recherche).

Notes

The authors declare no competing financial interest.

ACKNOWLEDGMENTS

The authors would like to acknowledge the Foundation Jean-Marie Lehn and the French Proteomic Infrastructure (ProFI) for support.

REFERENCES

- (1) Pal, L. B.; Bule, P.; Khan, W.; Chella, N. An Overview of the Development and Preclinical Evaluation of Antibody–Drug Conjugates for Non-Oncological Applications. *Pharmaceutics* **2023**, *15* (7), 1807.
- (2) Yao, P.; Zhang, Y.; Zhang, S.; Wei, X.; Liu, Y.; Du, C.; Hu, M.; Feng, C.; Li, J.; Zhao, F.; et al. Knowledge Atlas of Antibody–Drug Conjugates on CiteSpace and Clinical Trial Visualization Analysis. *Front. Oncol.* **2023**, *12*, 1039882.
- (3) Tarcsa, E.; Guffroy, M. R.; Falahatpisheh, H.; Phipps, C.; Kalvass, J. C. Antibody–Drug Conjugates as Targeted Therapies: Are We There yet? A Critical Review of the Current Clinical Landscape. *Drug Discovery Today: Technol.* **2020**, *37*, 13–22.
- (4) Fu, Z.; Li, S.; Han, S.; Shi, C.; Zhang, Y. Antibody Drug Conjugate: The “Biological Missile” for Targeted Cancer Therapy. *Signal Transduction Targeted Ther.* **2022**, *7* (1), 93.
- (5) Filleur, S.; Courtin, A.; Ait-Si-Ali, S.; Guglielmi, J.; Merle, C.; Harel-Bellan, A.; Clezardin, P.; Cabon, F. siRNA-Mediated Inhibition of Vascular Endothelial Growth Factor Severely Limits Tumor Resistance to Antiangiogenic Thrombospondin-1 and Slows Tumor Vascularization and Growth 1. *Cancer Res.* **2003**, *63* (14), 3919–3922.
- (6) Kumar, K.; Rani, V.; Mishra, M.; Chawla, R. New Paradigm in Combination Therapy of siRNA with Chemotherapeutic Drugs for Effective Cancer Therapy. *Curr. Res. Pharmacol. Drug Discov.* **2022**, *3*, 100103.
- (7) Sajid, M. I.; Moazzam, M.; Kato, S.; Yeseom Cho, K.; Tiwari, R. K. Overcoming Barriers for siRNA Therapeutics: From Bench to Bedside. *Pharmaceutics* **2020**, *13* (10), 294.
- (8) Salim, L.; Islam, G.; Desaulniers, J.-P. Targeted Delivery and Enhanced Gene-Silencing Activity of Centrally Modified Folic Acid–siRNA Conjugates. *Nucleic Acids Res.* **2020**, *48* (1), 75–85.
- (9) Nakamoto, K.; Akao, Y.; Furuichi, Y.; Ueno, Y. Enhanced Intercellular Delivery of cRGD–siRNA Conjugates by an Additional Oligospermine Modification. *ACS Omega* **2018**, *3* (7), 8226–8232.
- (10) Nakagawa, O.; Ming, X.; Huang, L.; Juliano, R. L. Targeted Intracellular Delivery of Antisense Oligonucleotides via Conjugation with Small-Molecule Ligands. *J. Am. Chem. Soc.* **2010**, *132* (26), 8848–8849.
- (11) Dassie, J. P.; Liu, X.; Thomas, G. S.; Whitaker, R. M.; Thiel, K. W.; Stockdale, K. R.; Meyerholz, D. K.; McCaffrey, A. P.; McNamara, J. O.; Giangrande, P. H. Systemic Administration of Optimized Aptamer-siRNA Chimeras Promotes Regression of PSMA-Expressing Tumors. *Nat. Biotechnol.* **2009**, *27* (9), 839–846.
- (12) Lu, H.; Wang, D.; Kazane, S.; Javahishvili, T.; Tian, F.; Song, F.; Sellers, A.; Barnett, B.; Schultz, P. G. Site-Specific Antibody–Polymer Conjugates for siRNA Delivery. *J. Am. Chem. Soc.* **2013**, *135* (37), 13885–13891.
- (13) Lorenzer, C.; Streußnig, S.; Tot, E.; Winkler, A.-M.; Merten, H.; Brandl, F.; Sayers, E. J.; Watson, P.; Jones, A. T.; Zangemeister-Wittke, U.; et al. Targeted Delivery and Endosomal Cellular Uptake of DARPIn-siRNA Bioconjugates: Influence of Linker Stability on Gene Silencing. *Eur. J. Pharm. Biopharm.* **2019**, *141*, 37–50.
- (14) Zhou, H.; Chen, D. S.; Hu, C. J.; Hong, X.; Shi, J.; Xiao, Y. Stimuli-Responsive Nanotechnology for RNA Delivery. *Adv. Sci.* **2023**, *10*, 2303597.
- (15) Liu, X.; Peng, L. Dendrimer Nanovectors for siRNA Delivery. *siRNA Delivery Methods: Methods in Molecular Biology*; Shum, K., Rossi, J., Eds.; Springer: New York, 2016; Vol. 1364, pp 127–142.
- (16) Mainini, F.; Eccles, M. R. Lipid and Polymer-Based Nanoparticle siRNA Delivery Systems for Cancer Therapy. *Molecules* **2020**, *25* (11), 2692.
- (17) Song, E.; Zhu, P.; Lee, S.-K.; Chowdhury, D.; Kussman, S.; Dykxhoorn, D. M.; Feng, Y.; Palliser, D.; Weiner, D. B.; Shankar, P.; et al. Antibody Mediated in Vivo Delivery of Small Interfering RNAs via Cell-Surface Receptors. *Nat. Biotechnol.* **2005**, *23* (6), 709–717.
- (18) Yang, J.; Sun, J.-F.; Wang, T.-T.; Guo, X.-H.; Wei, J.-X.; Jia, L.-T.; Yang, A.-G. Targeted Inhibition of Hantavirus Replication and Intracranial Pathogenesis by a Chimeric Protein-Delivered siRNA. *Antiviral Res.* **2017**, *147*, 107–115.
- (19) Kedmi, R.; Veiga, N.; Ramishetti, S.; Goldsmith, M.; Rosenblum, D.; Dammes, N.; Hazan-Halevy, I.; Nahary, L.; Leviatan-Ben-Arye, S.; Harlev, M.; et al. A Modular Platform for Targeted RNAi Therapeutics. *Nat. Nanotechnol.* **2018**, *13* (3), 214–219.
- (20) Bäumer, N.; Tiemann, J.; Scheller, A.; Meyer, T.; Wittmann, L.; Suburu, M. E. G.; Greune, L.; Peipp, M.; Kellmann, N.; Gumnior, A.; et al. Targeted siRNA Nanocarrier: A Platform Technology for Cancer Treatment. *Oncogene* **2022**, *41* (15), 2210–2224.
- (21) Pinel, S.; Aman, E.; Erblang, F.; Dietrich, J.; Frisch, B.; Sirman, J.; Kichler, A.; Sibling, A.-P.; Dontenwill, M.; Schaffner, F.; et al. Quantitative Measurement of Delivery and Gene Silencing Activities of siRNA Polyplexes Containing Pyridylthiourea-Grafted Polyethylenimines. *J. Controlled Release* **2014**, *182*, 1–12.
- (22) Chipper, M.; Tounsi, N.; Kole, R.; Kichler, A.; Zuber, G. Self-Aggregating 1.8 kDa Polyethylenimines with Dissolution Switch at Endosomal Acidic pH Are Delivery Carriers for Plasmid DNA, mRNA, siRNA and Exon-Skipping Oligonucleotides. *J. Controlled Release* **2017**, *246*, 60–70.
- (23) Lehot, V.; Neuberger, P.; Ripoll, M.; Daubeuf, F.; Erb, S.; Dovgan, I.; Ursuegui, S.; Cianféran, S.; Kichler, A.; Chaubet, G.; et al. Targeted Anticancer Agent with Original Mode of Action Prepared by Supramolecular Assembly of Antibody Oligonucleotide Conjugates and Cationic Nanoparticles. *Pharmaceutics* **2023**, *15* (6), 1643.

- (24) Lehot, V.; Kuhn, I.; Nothisen, M.; Erb, S.; Kolodych, S.; Cianfèrani, S.; Chaubet, G.; Wagner, A. Non-Specific Interactions of Antibody-Oligonucleotide Conjugates with Living Cells. *Sci. Rep.* **2021**, *11* (1), 5881.
- (25) Ripoll, M.; Neuberg, P.; Remy, J.-S.; Kichler, A. Cationic Photopolymerized Polydiacetylenic (PDA) Micelles for siRNA Delivery. *Nanotechnology for Nucleic Acid Delivery, Methods in Molecular Biology*; Ogris, M., Sami, H., Eds.; Springer: New York, 2019; Vol. 1943, pp 101–122.
- (26) Ripoll, M.; Neuberg, P.; Kichler, A.; Tounsi, N.; Wagner, A.; Remy, J.-S. pH-Responsive Nanometric Polydiacetylenic Micelles Allow for Efficient Intracellular siRNA Delivery. *ACS Appl. Mater. Interfaces* **2016**, *8* (45), 30665–30670.
- (27) Ripoll, M.; Pierdant, M.; Neuberg, P.; Bagnard, D.; Wagner, A.; Kichler, A.; Remy, J.-S. Co-Delivery of Anti-PLK-1 siRNA and Camptothecin by Nanometric Polydiacetylenic Micelles Results in a Synergistic Cell Killing. *RSC Adv.* **2018**, *8* (37), 20758–20763.
- (28) Perino, A.; Klymchenko, A.; Morere, A.; Contal, E.; Rameau, A.; Guenet, J.; Mély, Y.; Wagner, A. Structure and Behavior of Polydiacetylene-Based Micelles. *Macromol. Chem. Phys.* **2011**, *212* (2), 111–117.
- (29) Németh, Z.; Csóka, I.; Semnani Jazani, R.; Sipos, B.; Haspel, H.; Kozma, G.; Kónya, Z.; Dobó, D. G. Quality by Design-Driven Zeta Potential Optimisation Study of Liposomes with Charge Imparting Membrane Additives. *Pharmaceutics* **2022**, *14* (9), 1798.
- (30) Wilson, F. R.; Coombes, M. E.; Wylie, Q.; Yurchenko, M.; Brezden-Masley, C.; Hutton, B.; Skidmore, B.; Cameron, C. Herceptin® (trastuzumab) in HER2-positive early breast cancer: protocol for a systematic review and cumulative network meta-analysis. *Syst. Rev.* **2017**, *6* (1), 196.
- (31) Dovgan, I.; Ursuegui, S.; Erb, S.; Michel, C.; Kolodych, S.; Cianfèrani, S.; Wagner, A. Acyl Fluorides: Fast, Efficient, and Versatile Lysine-Based Protein Conjugation via Plug-and-Play Strategy. *Bioconjugate Chem.* **2017**, *28* (5), 1452–1457.
- (32) Strebhardt, K.; Ullrich, A. Targeting Polo-like Kinase 1 for Cancer Therapy. *Nat. Rev. Cancer* **2006**, *6* (4), 321–330.
- (33) Judge, A. D.; Robbins, M.; Tavakoli, I.; Levi, J.; Hu, L.; Fronda, A.; Ambegia, E.; McClintock, K.; MacLachlan, I. Confirming the RNAi-Mediated Mechanism of Action of siRNA-Based Cancer Therapeutics in Mice. *J. Clin. Invest.* **2009**, *119* (3), 661–673.
- (34) Rady, T.; Erb, S.; Deddouche-Grass, S.; Morales, R.; Chaubet, G.; Cianfèrani, S.; Basse, N.; Wagner, A. Targeted Delivery of Immune-Stimulating Bispecific RNA, Inducing Apoptosis and Anti-Tumor Immunity in Cancer Cells. *iScience* **2024**, *27* (3), 109068.